SENESCENZA INDOTTA DA ONCOGENI

Vie diverse inducono senescenza

MOLECULAR AND CELLULAR BIOLOGY, July 2002, p. 5157–5172 Vol. 22, No. 14
0270-7306/02/$04.00+0 DOI: 10.1128/MCB.22.14.5157–5172.2002

A Two-Stage, p16^{INK4A}- and p53-Dependent Keratinocyte Senescence Mechanism That Limits Replicative Potential Independent of Telomere Status†

James G. Rheinwald,[1,2]* William C. Hahn,[3,4,5] Matthew R. Ramsey,[1,2] Jenny Y. Wu,[1,2] Zongyou Guo,[1,2] Hensin Tsao,[6] Michele De Luca,[7] Caterina Catricalà,[8] and Kathleen M. O'Toole[1,2]

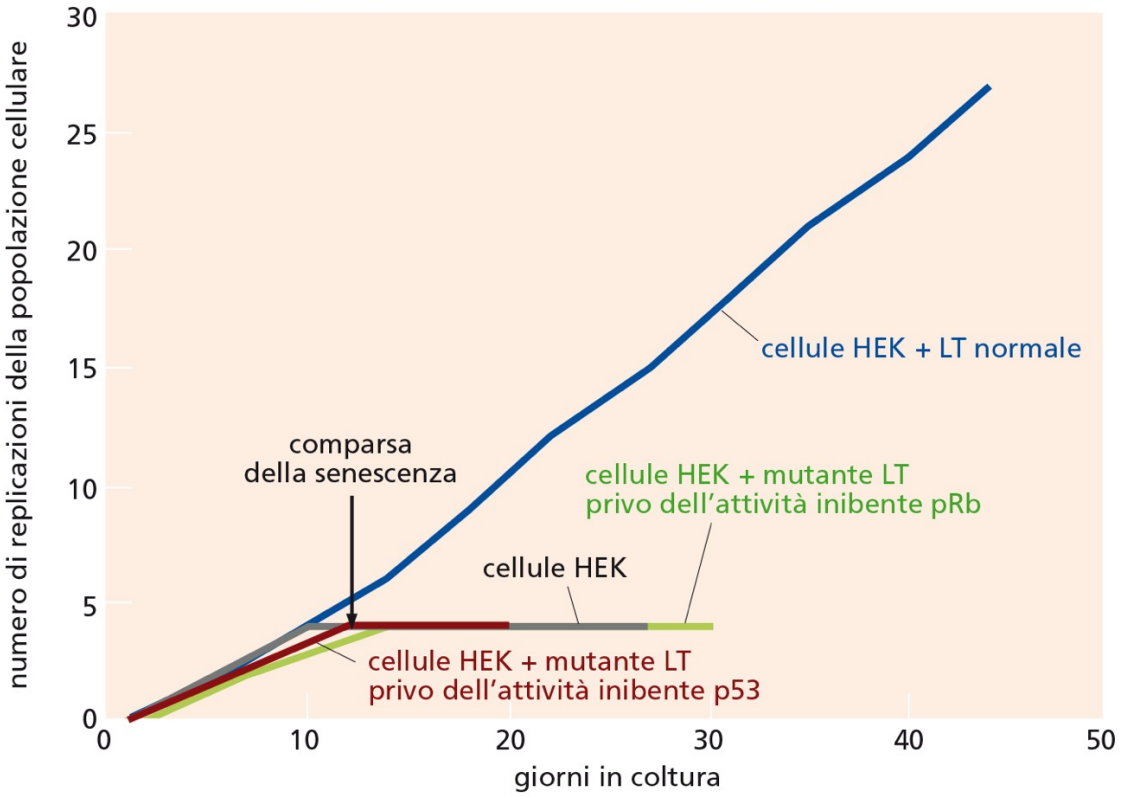

Espressione Large T antigen (LT) di SV40 selvatico o mutante in cellule embrionali di rene (HEK)

Weinberg, la biologia del cancro

Senescenza indotta da oncogeni

Cell, Vol. 88, 593–602, March 7, 1997, Copyright ©1997 by Cell Press

Oncogenic *ras* Provokes Premature Cell Senescence Associated with Accumulation of p53 and p16^{INK4a}

Manuel Serrano,*†‡ Athena W. Lin,* Mila E. McCurrach,* David Beach,*† and Scott W. Lowe*
*Cold Spring Harbor Laboratory
†Howard Hughes Medical Institute
Cold Spring Harbor, New York 11724

Vol 444|30 November 2006|doi:10.1038/nature05268 nature

LETTERS

Oncogene-induced senescence is part of the tumorigenesis barrier imposed by DNA damage checkpoints

Jirina Bartkova[1]*, Nousin Rezaei[2]*, Michalis Liontos[3]*, Panagiotis Karakaidos[3], Dimitris Kletsas[4], Natalia Issaeva[5], Leandros-Vassilios F. Vassiliou[3], Evangelos Kolettas[6], Katerina Niforou[3], Vassilis C. Zoumpourlis[7], Munenori Takaoka[8], Hiroshi Nakagawa[8], Frederic Tort[1], Kasper Fugger[1], Fredrik Johansson[5], Maxwell Sehested[9], Claus L. Andersen[10], Lars Dyrskjot[10], Torben Ørntoft[10], Jiri Lukas[1], Christos Kittas[3], Thomas Helleday[5,11], Thanos D. Halazonetis[2,12], Jiri Bartek[1] & Vassilis G. Gorgoulis[3]

Serrano et al., 1997; Bartkova et al., 2006

Senescenza indotta da oncogeni

Cell lines:
-primary (presenescent) human diploid fibroblasts (IMR90 and WI38),
-primary mouse embryo fibroblasts (MEFs)
-rat REF52 cell line.

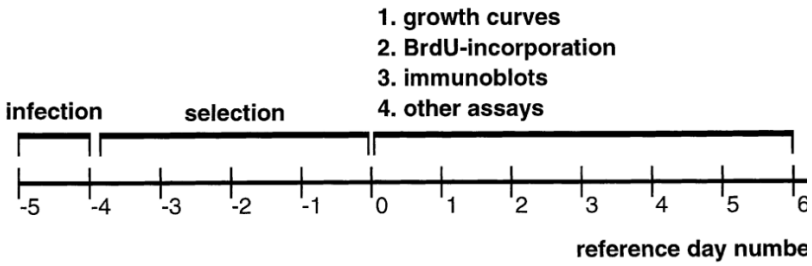

Figure 1. Experimental Design and Reference Time Frame

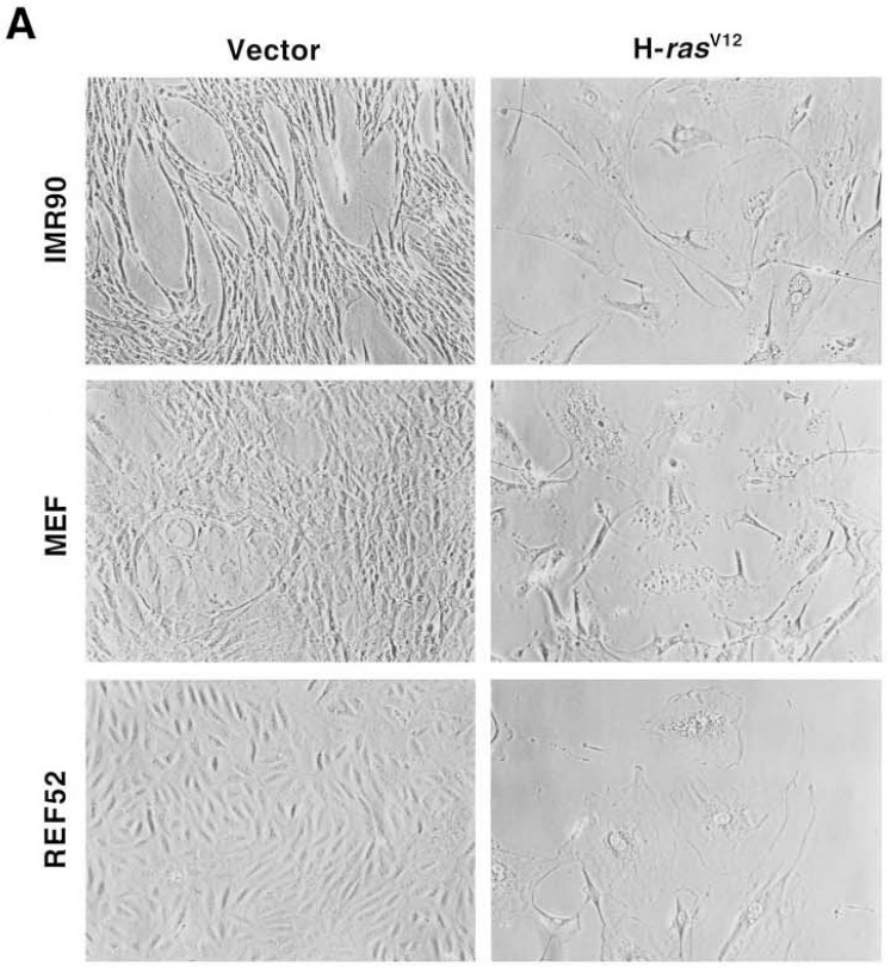

Serrano et al., 1997

Senescenza indotta da oncogeni

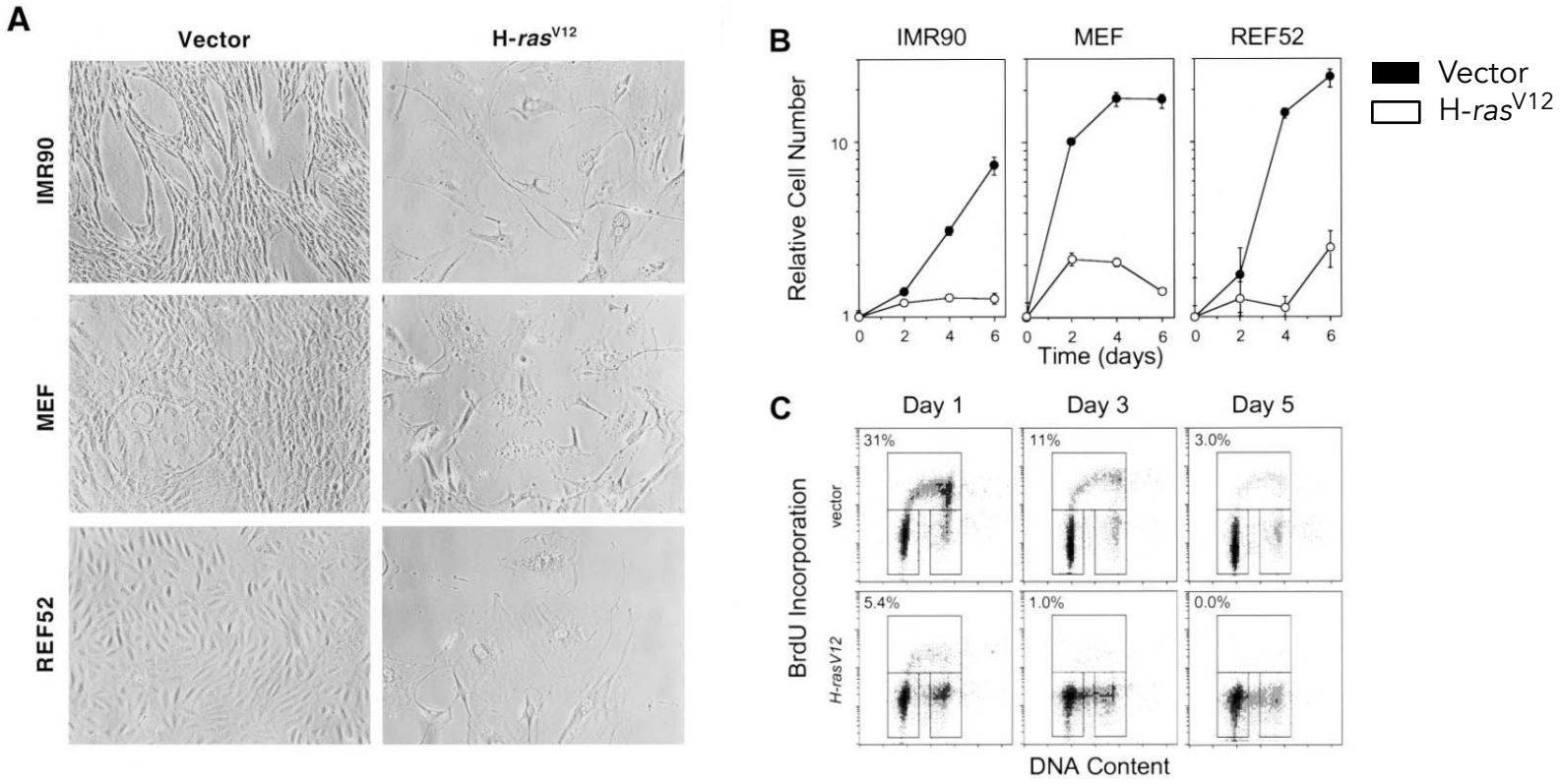

Figure 2. Effect of H-*ras*V12 on Primary Fibroblasts

The indicated cell-types were transduced with retroviruses expressing H-*ras*V12 or with empty-vector control (pBabe-Puro).
(A) Cell morphology at day 6. Photographs are at the same magnification.
(B) Representative growth curves corresponding to the indicated cell cultures transduced with empty vector (closed circles) or with H-*ras*V12-expressing (open circles) retroviruses. The time frame corresponds to the scheme in Figure 1. Each curve was performed at least twice, and each time point was determined in triplicate.
(C) Cell-cycle distribution of H-*ras*V12-expressing and control populations as measured by BrdU incorporation and DNA-content flow cytometry analysis. Cells were stained with FITC-anti-BrdU to detect BrdU incorporation (vertical axis) and propidium iodide to detect total DNA (horizontal axis). The upper box identifies cells incorporating BrdU (~S phase), the lower-left box identifies G0/G1 cells, and the lower-right box displays G2/M cells. The percentage of cells incorporating BrdU is indicated in the upper left of each graph.

Serrano et al., 1997

Senescenza indotta da oncogeni

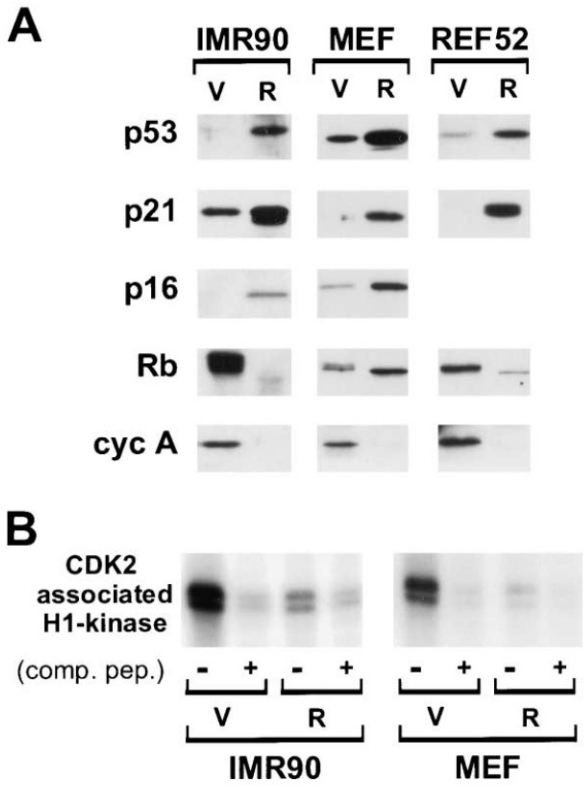

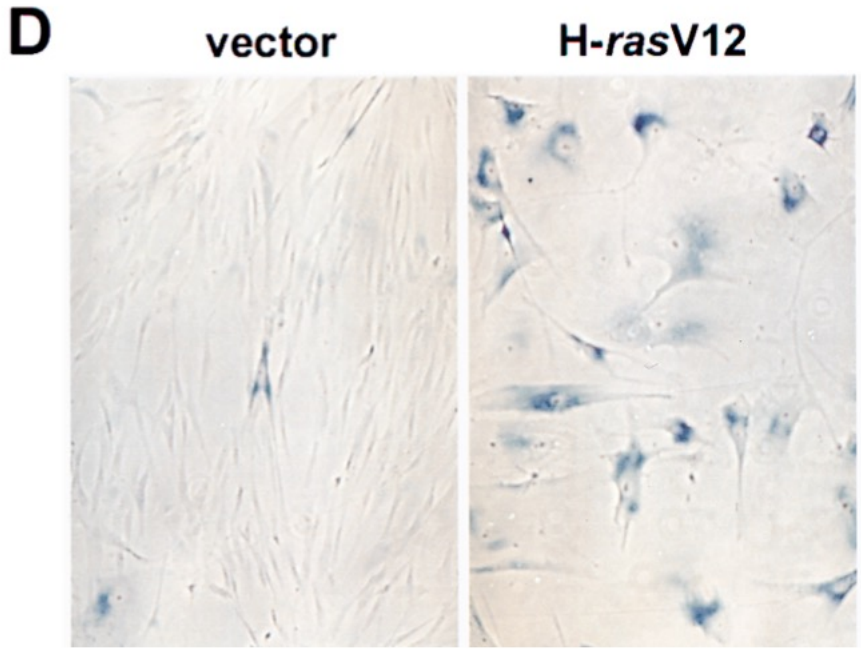

Figure 3. Effect of H-*ras*V12 on Cell-Cycle Regulatory Proteins

(A) Immunoblots of cellular lysates corresponding to cells transduced with empty vector (V) or with H-*ras*V12-expressing (R) retroviruses. Our anti-p16 antibodies did not crossreact with rat p16, so we could not examine p16 expression in REF52 cells.

(B) CDK2 kinase activity against histone H1 obtained after immunoprecipitation of the indicated cellular lysates, (V) or (R) as in (A), with anti-CDK2 in the absence (−) or presence (+) of competing antigenic peptide.

Serrano et al., 1997

Senescenza indotta da oncogeni

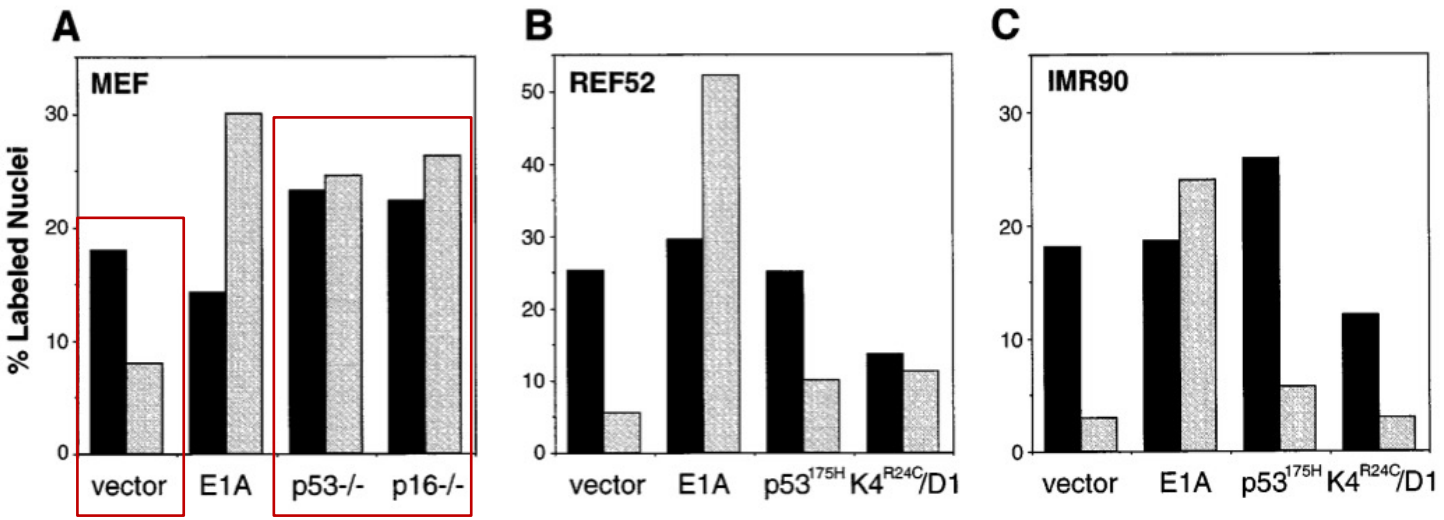

Vector

H-*ras*^{V12}

$p53^{175H}$ = dominant-negative p53 mutant

$CDK4^{R24C}$ = mutant CDK4 protein insensitive to p16

Figure 5. Genetic Analysis of H-*ras*V12-Induced Arrest: BrdU Incorporation at Day 2

The indicated cell types were transduced with empty vector (solid bars) or with H-*ras*V12-expressing (shaded bars) retroviruses. BrdU incorporation was detected by immunofluorescence. The average of two experiments is shown, and at least 200 cells were counted per experiment.

(A) Mouse embryo fibroblasts (MEF) of wild-type genotype containing empty vector or expressing E1A, MEF-*p53*$^{-/-}$, or MEF-*p16*$^{-/-}$, as indicated.

(B) REF52 cells containing empty vector or expressing the indicated proteins.

(C) IMR90 cells containing empty vector or expressing the indicated proteins.

Serrano et al., 1997

Senescenza e Cancro

INNOVATION

The power and the promise of oncogene-induced senescence markers

Manuel Collado and Manuel Serrano

Senescence: irreversible proliferate arrest of cells caused by various stresses

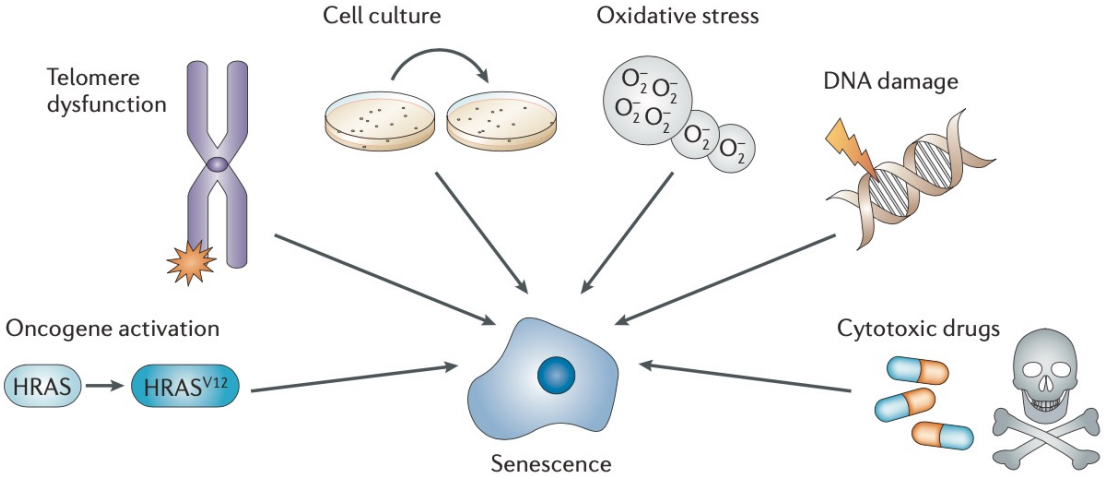

Figure 1 | **Many roads to senescence.** Diverse factors can engage a common programme the end point of which is the establishment of an irreversible proliferative arrest known as senescence. All of these stimuli represent stressful conditions for the cell, many of which are present in the tumour environment. Senescence functions as a self-defence mechanism to prevent the proliferation of potentially damaged cells. In some instances, the same stimulus might induce either senescence or apoptosis, but the mechanisms that govern the decision to engage one or the other are not known.

Collado and Serrano, 2006

Senescenza e Cancro

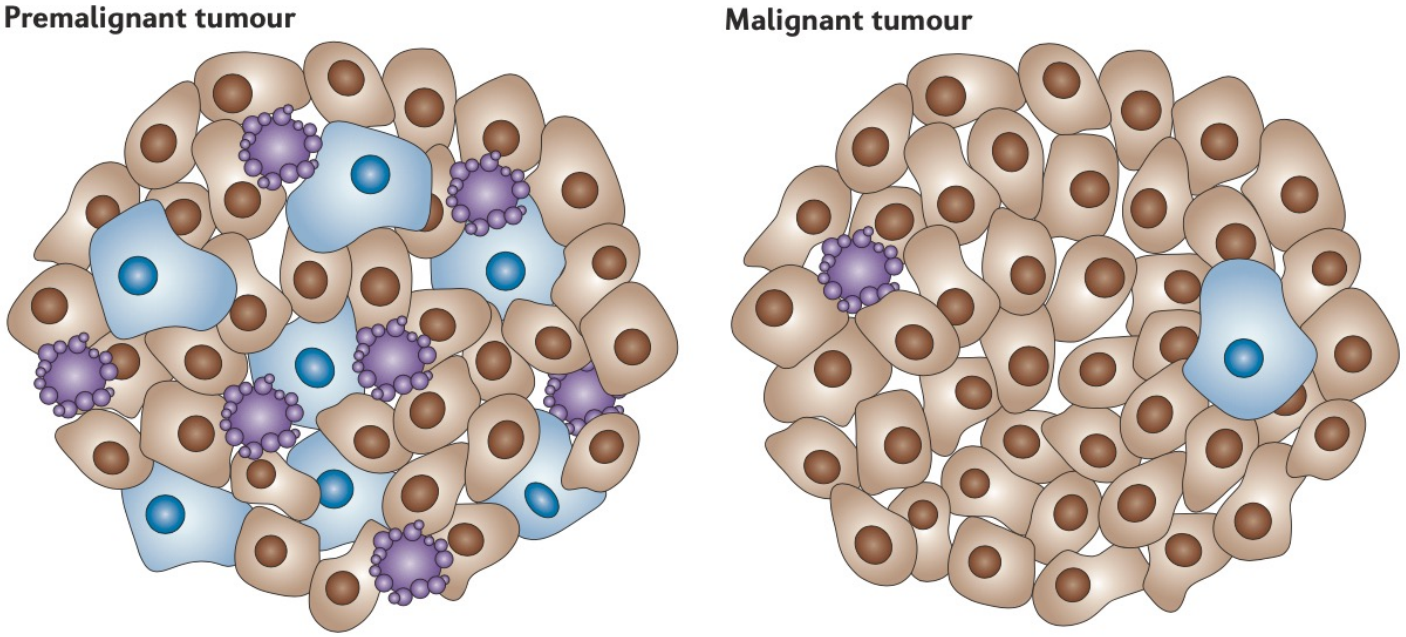

Figure 2 | **Senescence in premalignant neoplastic lesions.** A heterogeneous population of tumour cells is a characteristic of premalignant tumours. Therefore, it is possible to identify the cells that undergo apoptosis (shown in purple) or senescence (shown in blue) within premalignant lesions. These cells are probably responsible for the restriction of the growth of these lesions. By contrast, in most malignant tumours, the balance between proliferating (shown in brown) versus apoptotic and senescent cells is altered in favour of proliferation and, therefore, tumour progression.

Collado and Serrano, 2006

Senescenza indotta da oncogeni e Cancro

Senescenza

Tumorigenesi

Ras oncogene

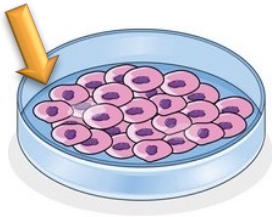

Senescence

Inducible
tissue-specific
Ras oncogene

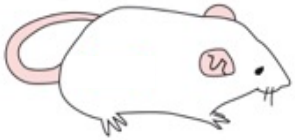

Iperplasia

Cell senescenti rilasciano
citochine pro-infiammatorie
anche per settimane

Tumor
progression

CRISI E APOPTOSI

Senescenza vs crisi

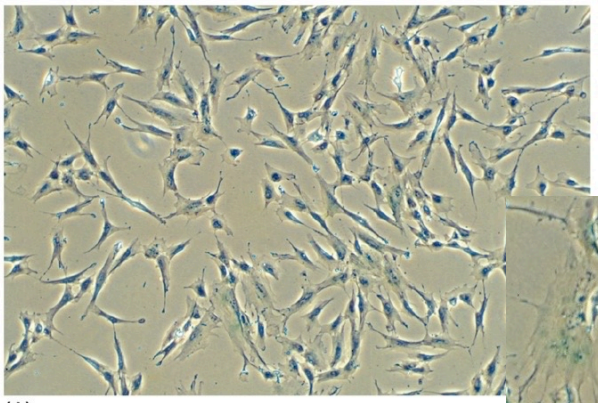
(A)

Senescenza: cellule vitali, cariotipo relativamente stabile

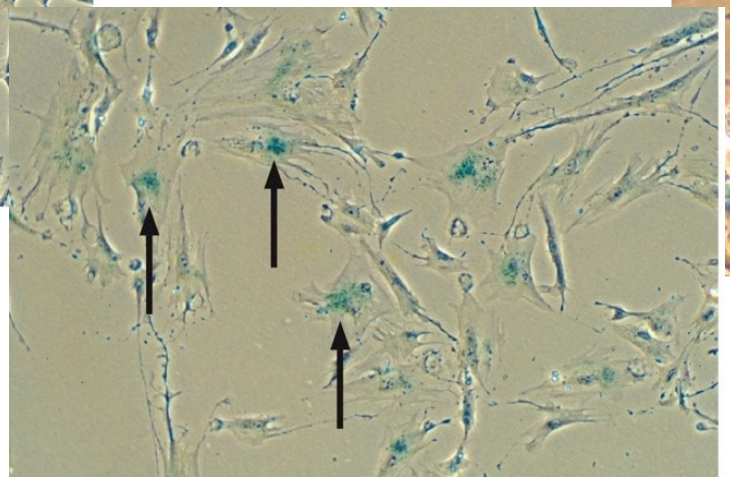

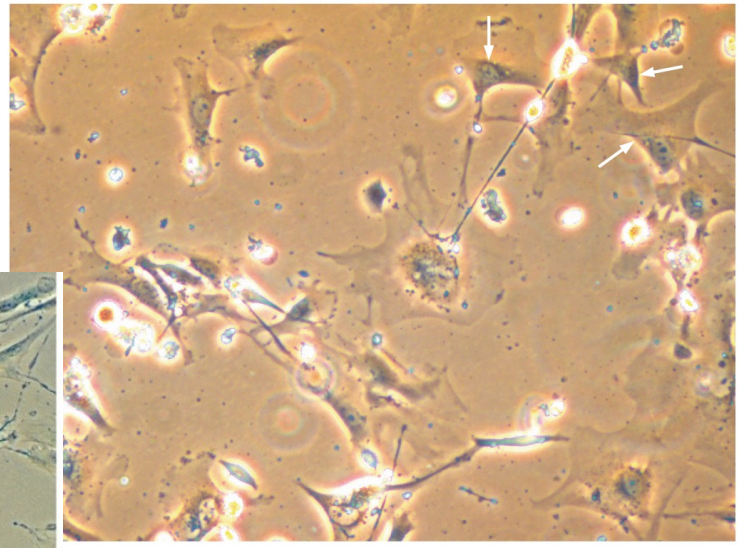

Crisi: cellule in apoptosi; cariotipo instabile

Weinberg, la biologia del cancro

Senescenza vs crisi

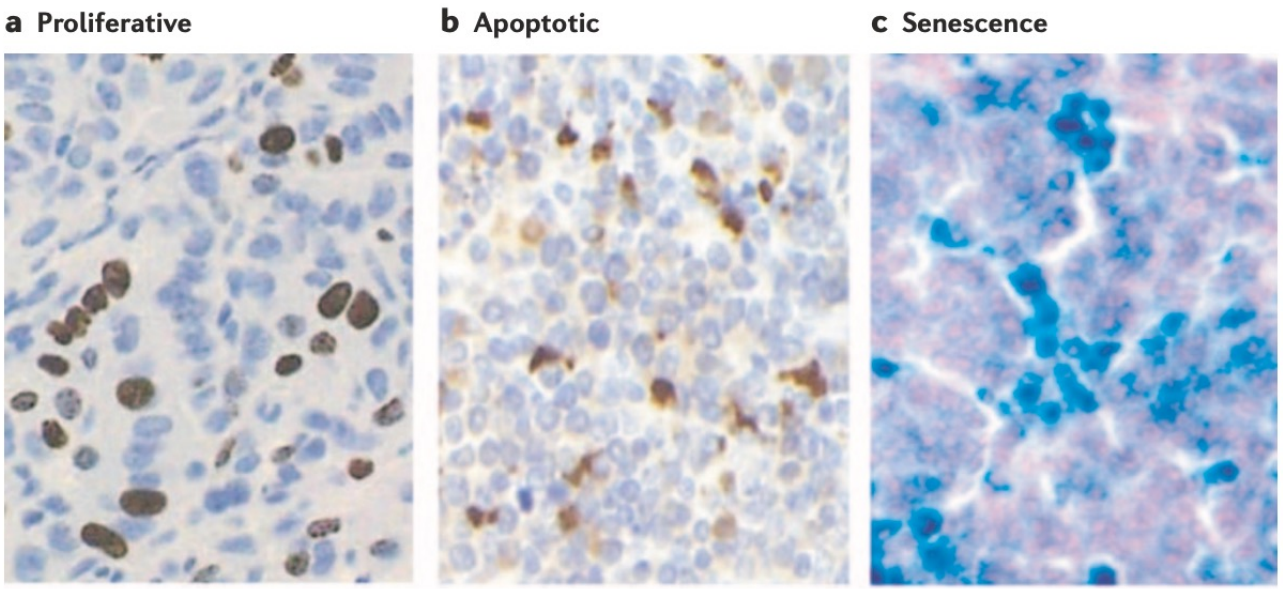

Figure 3 | **Senescence index.** Tumours can be assayed using different markers for the presence of cells that are actively proliferating (for example, using Ki67 staining), undergoing apoptosis (for example, active caspase-3 staining) or undergoing senescence (for example, using senescence-associated β-galactosidase (SA-β-Gal) staining). An 'index' could be derived from the results of these assays and would represent the percentage of cells within a tumour that are part of the pro-malignant state ('proliferative index'; brown cells (**a**)), together with the percentage of cells that restrict tumour growth, represented by apoptosis ('apoptotic index'; brown cells (**b**)) or senescence ('senescence index'; blue cells (**c**)). The images are intended only for illustrative purposes and are not from the same tumour.

Due meccanismi diversi!

Collado and Serrano, 2006

I TELOMERI

I telomeri

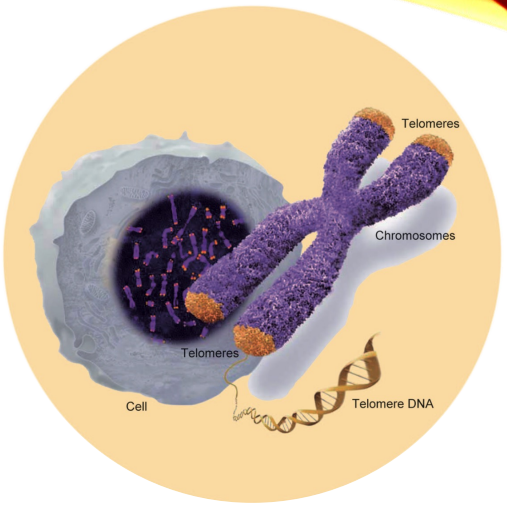

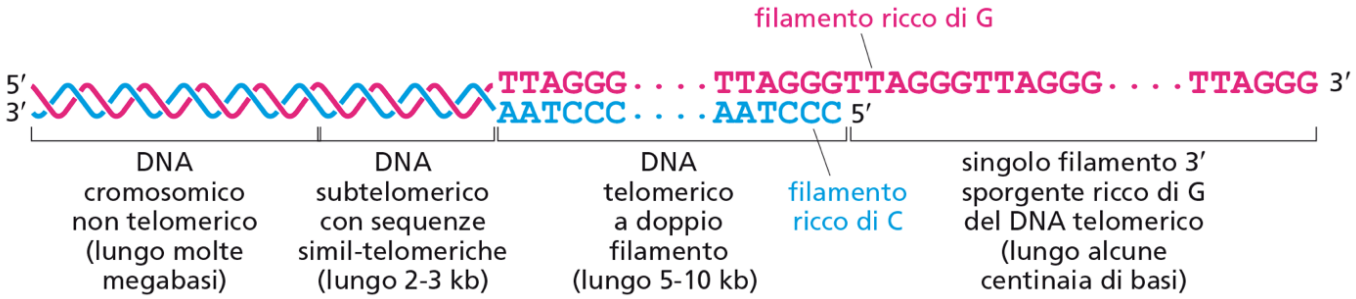

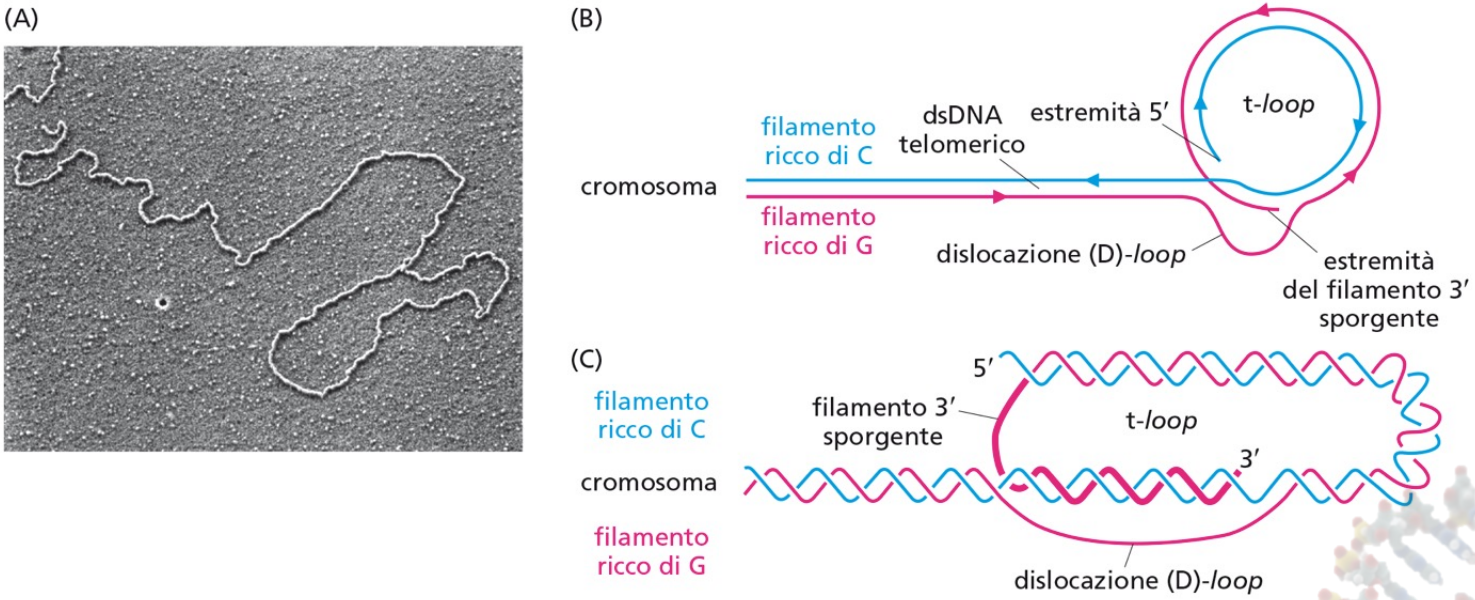

Weinberg, la biologia del cancro; Szostak

Human telomere

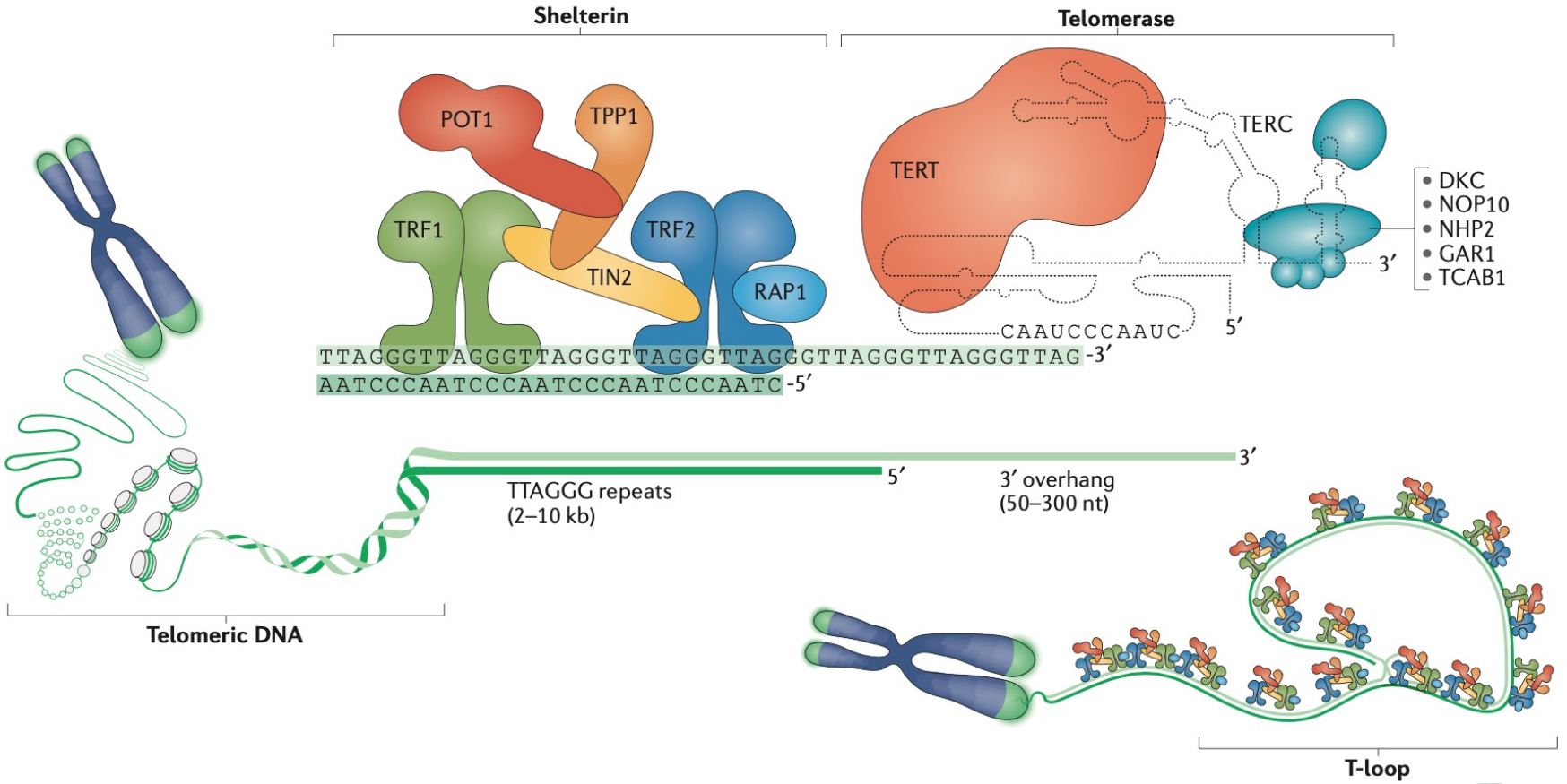

De Lange, 2018; Maciejowski and de Lange, 2017

Telomeri e crisi

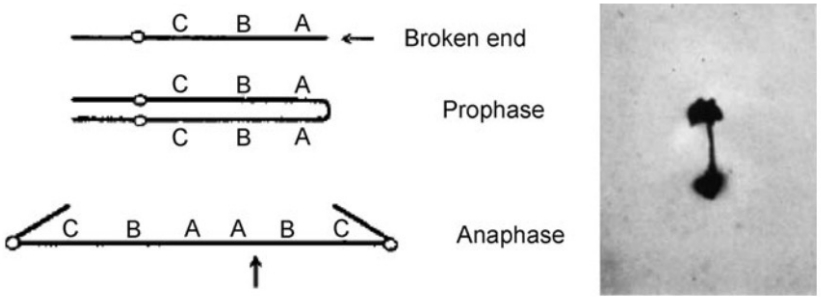

Figure 1. The chromosomal breakage-fusion-bridge cycle explored by Barbara McClintock. Left: After the replication of a broken chromosome, the two broken ends join together, creating a dicentric chromosome. When the two centromeres are pulled to opposite poles of the dividing cell, the chromosome breaks, and the new broken chromosomes continue the cycle (*Genetics*, **1941**, *26*, 234–282). Right: micrograph of a dicentric chromosome bridging the two poles of a mitotic spindle (*Genetics*, **1938**, *23*, 315–376).

FISH con sonda per ripetizioni telomeriche

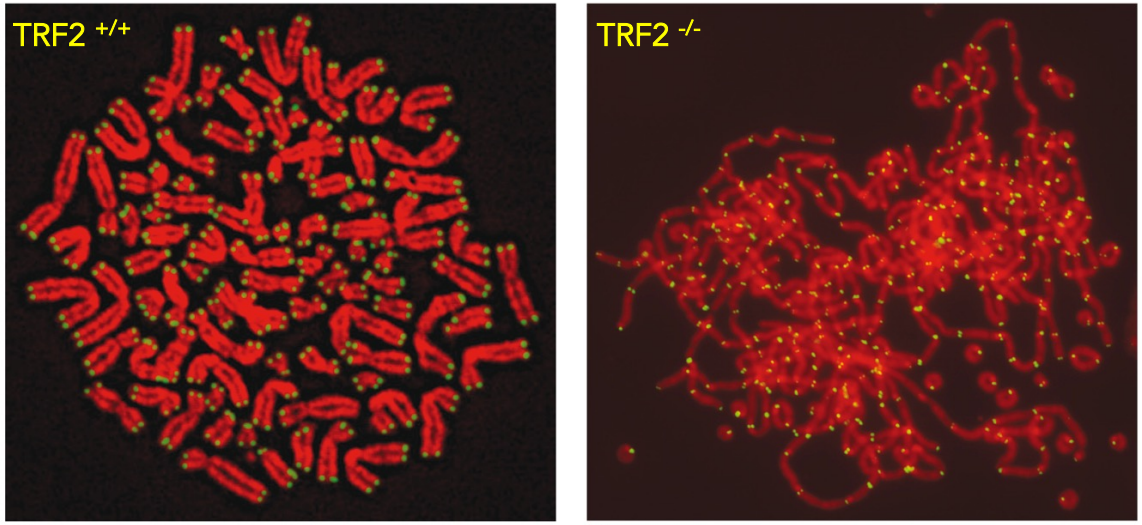

Weinberg, la biologia del cancro; Szostak et al., 2010

Telomeri e crisi

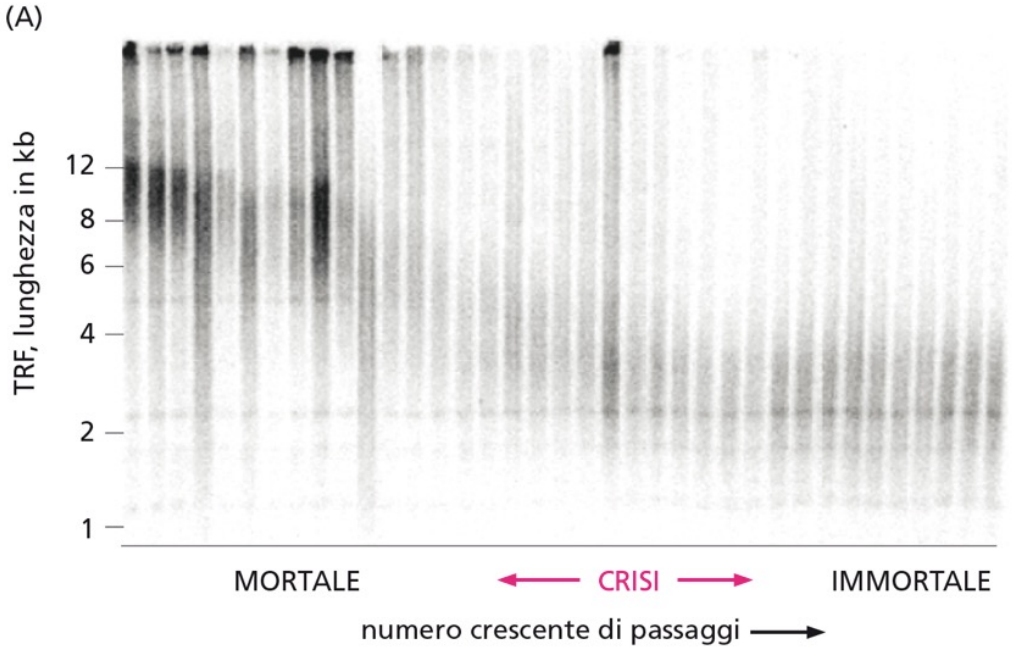

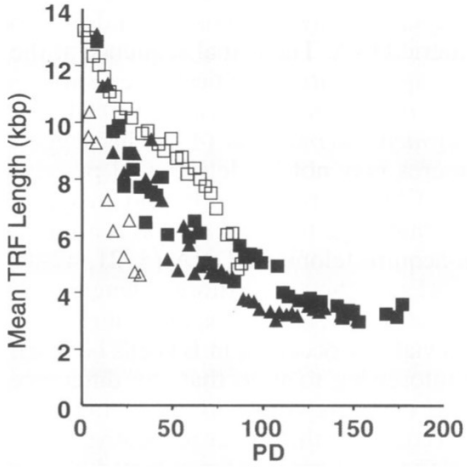

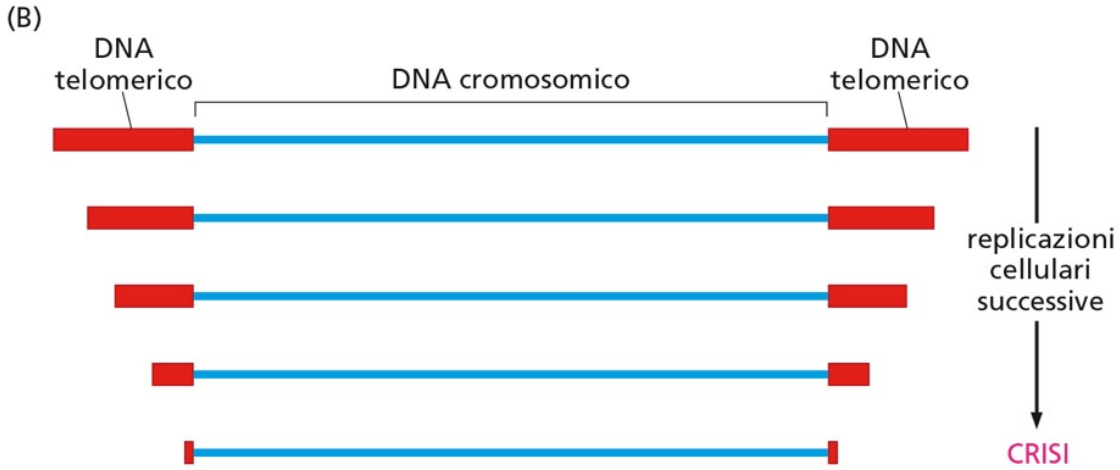

Weinberg, la biologia del cancro; Counter et al., 1994

Telomeri e crisi

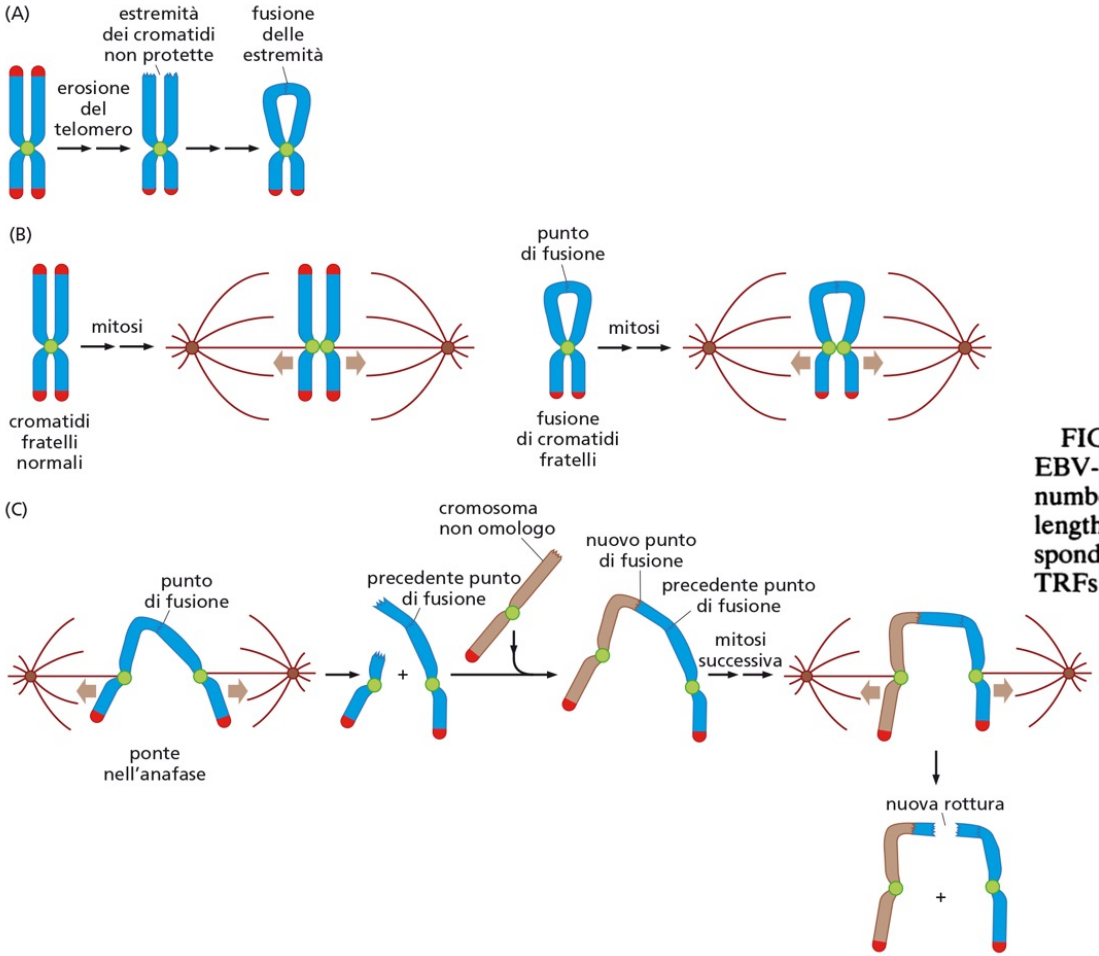

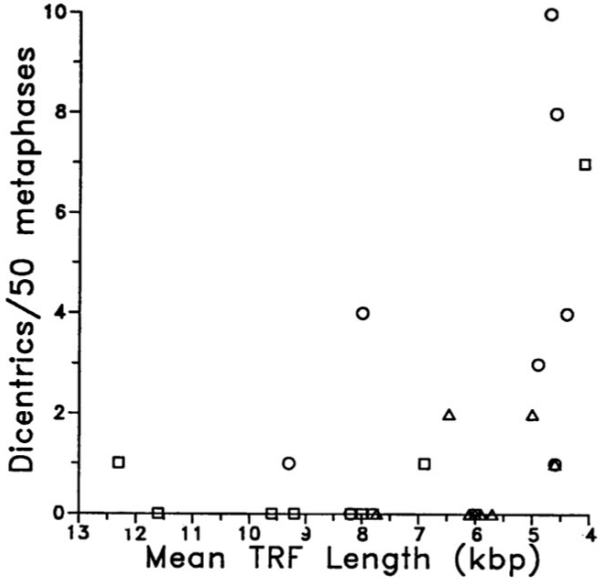

FIG. 3. Dicentrics per 50 metaphases versus mean TRF length in EBV-transformed B lymphocytes: B5 (□), B4 (△), and B3 (○). The number of dicentrics detected at crisis, when TRFs are 4 to 5 kbp in length, was found to be significantly different from the values corresponding to TRFs 1 kbp longer (5 to 6 kbp; $P = 0.004$) or to all larger TRFs (up to 13 kbp; $P < 0.0001$).

Weinberg, la biologia del cancro; Counter et al., 1994

Telomeri e crisi

Chromosoma (2006) 115:459–467
DOI 10.1007/s00412-006-0074-4

RESEARCH ARTICLE

The breakage–fusion–bridge (BFB) cycle as a mechanism for generating genetic heterogeneity in osteosarcoma

Shamini Selvarajah · Maisa Yoshimoto · Paul C. Park · Georges Maire · Jana Paderova · Jane Bayani · Gloria Lim · Khaldoun Al-Romaih · Jeremy A. Squire · Maria Zielenska

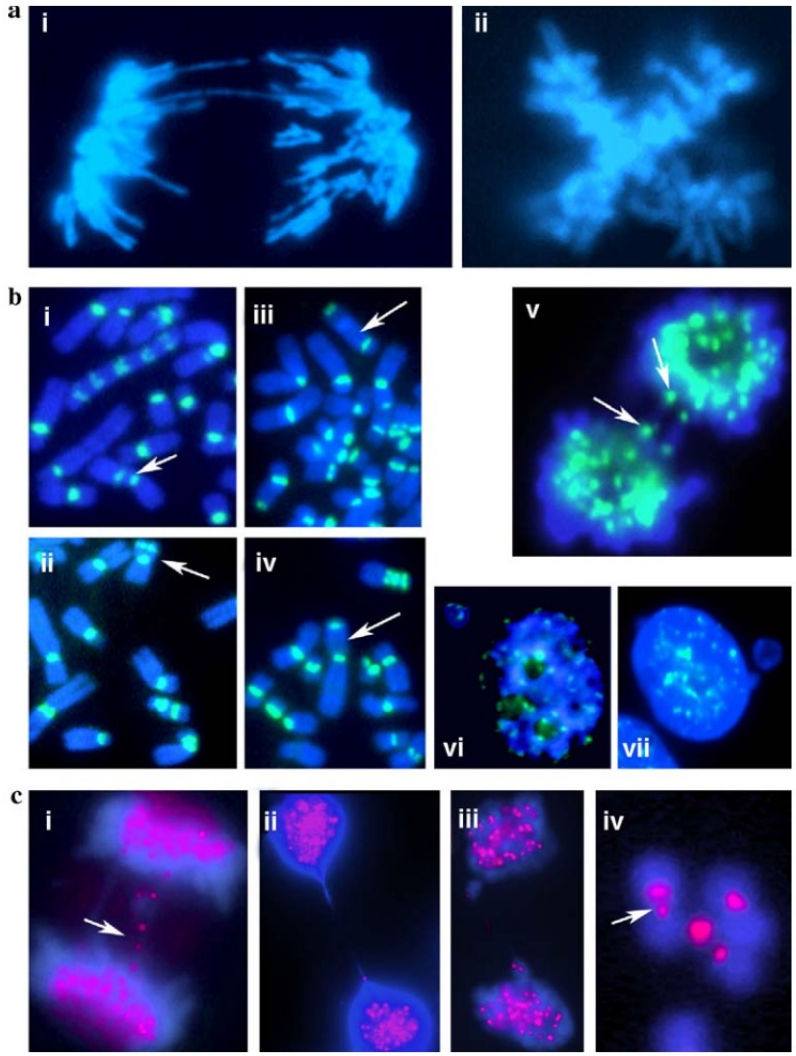

Fig. 1 Chromosomal instability in U-2 OS, HOS, MG-63, and SAOS-2 cell lines. **a***1* Chromatid bridge showing a perpendicular filamentous connection linking two aligned plates, *2* multipolar mitotic figure. **b** Alpha-satellite staining. *1–4* Dicentric chromosomes visualized by PNA FISH for alpha-satellite repeats in all the OS cell lines (*white arrows*); *5* dual PNA FISH signals for the alphoid repeats in the chromatin strings of anaphase bridges (*white arrows*); *6* micronuclei with staining for alphoid repeats; *7* micronuclei negative for the alphoid repeats (acentric). **c** Active centromere staining. *1* Multiple signals for CENP-A were visualized along the chromatin string (*white arrows*). *2* Internuclear string at telophase with a signal for CENP-A at one end, while *3* shows protrusions exhibiting signals in these blebs. *4* Enlargement of a functional dicentric with two signals for the kintetochore complex (*white arrow*; CREST antibodies)

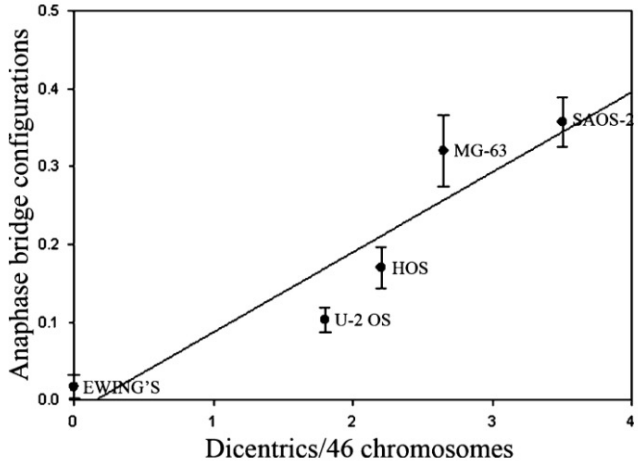

Fig. 2 Correlation between dicentric/multicentric chromosomes and anaphase bridge configurations. A positive correlation was found between the number of dicentrics/multicentrics per metaphase and ABC among the OS cell lines. ABC frequencies are displayed on the *y-axis*, while the number of dicentric/multicentric chromosomes is shown on the *x-axis*. The number of dicentrics was expressed as a ratio where the total number of chromosomes within each of the 40 metaphases counted was used as a denominator. This ratio was then multiplied by 46 to derive a representative measure of the degree of mitotic instability for each cell line relative to the normal chromosomal complement. Correlation is shown with regression analysis using Sigmaplot v9.0. The Pearson correlation coefficient is 0.929. The *p* value is 0.0222

Weinberg, la biologia del cancro; Counter et al., 1994

Telomeri e crisi

Chromosomal breakage-fusion-bridge events cause genetic intratumor heterogeneity

David Gisselsson*†, Louise Pettersson*, Mattias Höglund*, Markus Heidenblad*, Ludmila Gorunova*, Joop Wiegant‡, Fredrik Mertens*, Paola Dal Cin§¶, Felix Mitelman*, and Nils Mandahl*

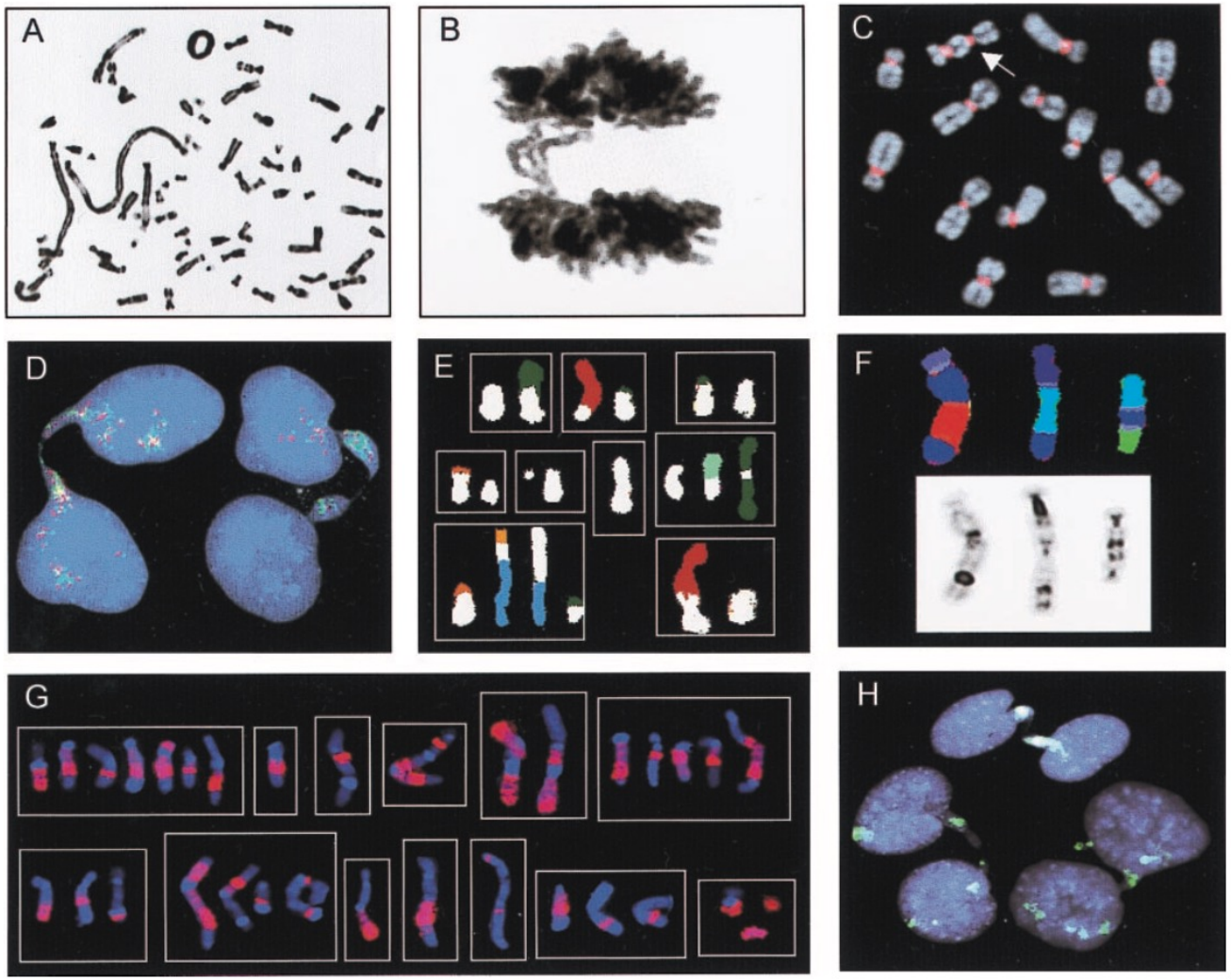

Weinberg, la biologia del cancro; Gisselsson et al., 2000

The end-replication problem

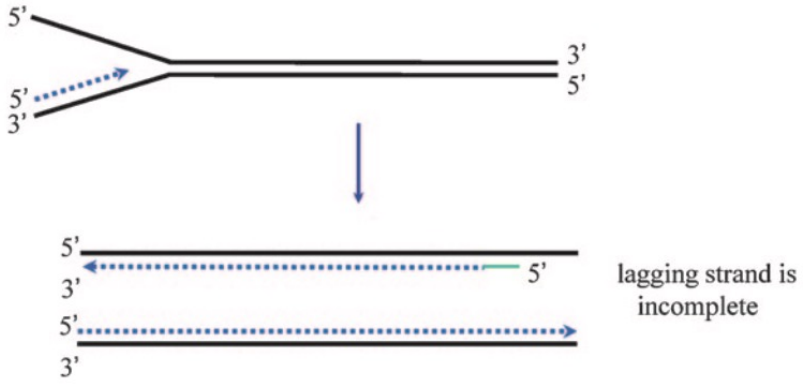

Figure 2. The end-replication problem as posed by Watson[18] and by Olovnikov.[19] When a replication fork reaches the end of a chromosome, the lagging strand will necessarily be incomplete as a result of the removal and potentially internal location of the last primer generated by primase.

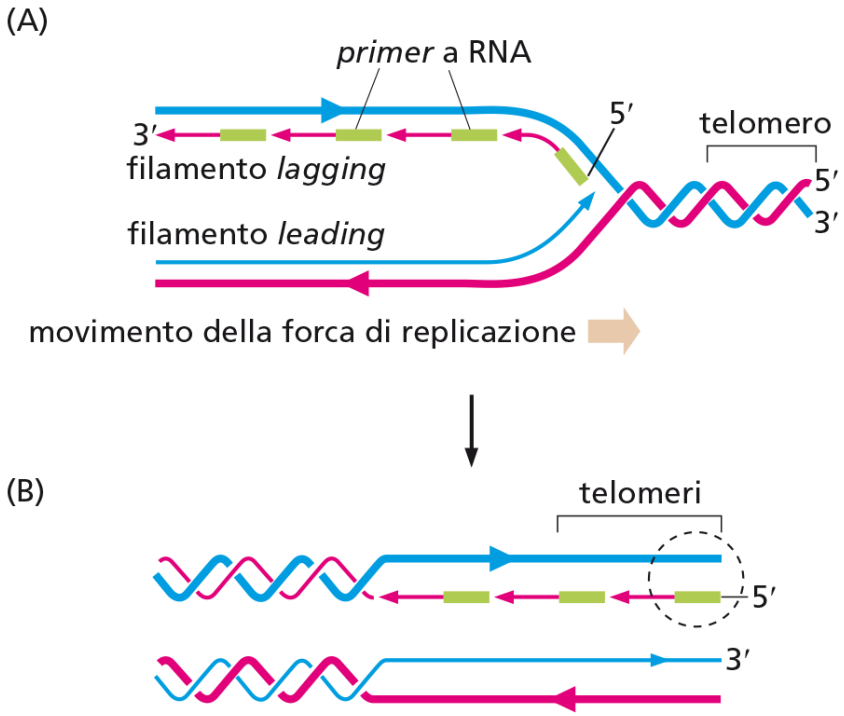

Weinberg, la biologia del cancro